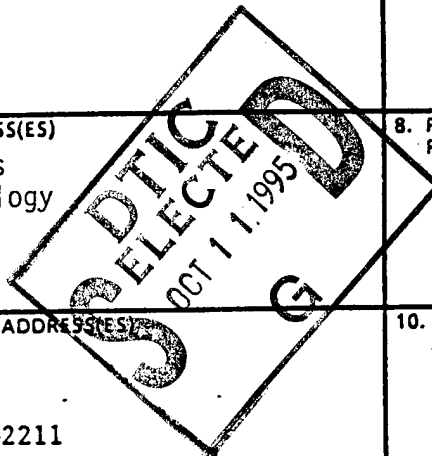


REPORT DOCUMENTATION PAGE			Form Approved OMB No. 0704-0188	
<small>Public reporting burden for this collection of information is estimated to average 1 hour per response, including the time for reviewing instructions, searching existing data sources, gathering and maintaining the data needed, and completing and reviewing the collection of information. Send comments regarding this burden estimate or any other aspect of this collection of information, including suggestions for reducing this burden, to Washington Headquarters Services, Directorate for Information Operations and Reports, 1215 Jefferson Davis Highway, Suite 1204, Arlington, VA 22202-4302, and to the Office of Management and Budget, Paperwork Reduction Project (0704-0188), Washington, DC 20503.</small>				
1. AGENCY USE ONLY (Leave blank)	2. REPORT DATE 7/13/95	3. REPORT TYPE AND DATES COVERED Final 5/1/92 - 4/30/95		
4. TITLE AND SUBTITLE New Developments in Atom Interferometry		5. FUNDING NUMBERS DAAL03-92-G-0229		
6. AUTHOR(S) Dr. David Pritchard		30141-PH		
7. PERFORMING ORGANIZATION NAME(S) AND ADDRESS(ES) Research Laboratory of Electronics Massachusetts Institute of Technology 77 Massachusetts Avenue Cambridge, MA 02139-4307		8. PERFORMING ORGANIZATION REPORT NUMBER		
9. SPONSORING/MONITORING AGENCY NAME(S) AND ADDRESS(ES) U. S. Army Research Office P. O. Box 12211 Research Triangle Park, NC 27709-2211		10. SPONSORING/MONITORING AGENCY REPORT NUMBER		
11. SUPPLEMENTARY NOTES The view, opinions and/or findings contained in this report are those of the author(s) and should not be construed as an official Department of the Army position, policy, or decision, unless so designated by other documentation.				
12a. DISTRIBUTION/AVAILABILITY STATEMENT Approved for public release; distribution unlimited.			12b. DISTRIBUTION CODE	
13. ABSTRACT (Maximum 200 words) Work by Prof. Pritchard and his collaborators is summarized here				
14. SUBJECT TERMS			15. NUMBER OF PAGES	
			16. PRICE CODE	
17. SECURITY CLASSIFICATION OF REPORT UNCLASSIFIED	18. SECURITY CLASSIFICATION UNCLASSIFIED	19. SECURITY CLASSIFICATION OF ABSTRACT UNCLASSIFIED	20. LIMITATION OF ABSTRACT UL	



19951006 004

DTIC QUALITY INSPECTED R

**Final ARO Report**  
**New Developments in Atom Interferometry**

**Grant No.: DAAL03-92-G-.0229**

**May 1, 1992 through April 30, 1995**

Accession For	
NTIS CRA&I	<input checked="" type="checkbox"/>
DTIC TAB	<input type="checkbox"/>
Unannounced	<input type="checkbox"/>
Justification .....	
By .....	
Distribution /	
Availability Codes	
Dist	Avail and/or Special
A-1	

## Table of Contents

1. Introduction .....	1
2. Results from previous support .....	1
2.A. Apparatus & Techniques .....	1
2.B. Experiments .....	3
2.B.1. Accurate Atomic Polarizability .....	3
2.B.2. Index of Refraction .....	4
2.B.3. Molecule Interferometry .....	6
2.B.4. Contrast Interferometry .....	6
2.B.5. Decoherence experiment .....	6
2.B.6. Regained coherence through greater selectivity .....	8
3. Publications and Theses .....	10
3.A. Recent papers published or submitted: .....	10
3.B. Theses: .....	11
4. Scientific Personnel .....	12
6. Bibliography .....	13

## List of Figures

**Figure 1.** A schematic, not to scale, of our atom interferometer.

**Figure 2.** Phase shift of the interference pattern as a function of voltage applied to the left (open circles) or right (filled circles) side of the interaction region. The fit is to a quadratic and the residuals are shown in the lower graph.

**Figure 3.** Phase shift of Na matter waves plotted vs. the interfering amplitude when passing through He, Ne and Ar in the gas cell. The slope of the fitted line is a direct measurement of the ratio  $\text{Re}(f(k,0)) / \text{Im}(f(k,0))$ .

**Figure 4.** Relative contrast and phase shift of the IFM as a function of the separation of the IFM arms at the point of scattering. The inset shows the angular distribution of spontaneously emitted photons projected onto the  $x$  axis. The dashed curve corresponds to purely single photon scattering, and the solid curve is a best fit that includes contributions from atoms that scattered 0 photons (4%) and 2 photons (14%).

**Figure 5.** Relative contrast and phase shift of the IFM as a function of  $d$  for the cases in which atoms are correlated with photons scattered into a limited range of directions. The dashed curve is for the uncorrelated case. The inset shows the acceptance of the detector for each case compared to the original distribution (dotted line). Case I corresponds to predominantly forward scattered photons (minimal transfer of momentum), case III corresponds to backward scattered photons (transfer of 2 photon momenta), and case II lies in between.

## 1. Introduction

Atom interferometers may well be the most important development in atomic physics in the 1990's. Following the near simultaneous demonstration of four atom interferometers in 1991 [CAM91, KAC91, KET91, RKW91], intense activity has been devoted to developing better atom beamsplitters [ASM94] and some effort has been devoted to applying these instruments to the wide range of fundamental and applied scientific problems for which they are so well suited.

In the current grant period we have developed our atom interferometer and used it to perform several novel measurements in atomic and molecular physics and also to address several fundamental questions in quantum mechanics.

## 2. Results from previous support

Our progress during the grant period has been considerable, culminating in 18 papers published or submitted as well as four Ph. D. and B. S. theses. These are listed in Sec. 3. This work reflects six different experiments that probe issues in atomic and molecular physics and in quantum mechanics which we summarize below. These experiments required a much improved 3-grating interferometer, similar to the first true atom interferometer that we demonstrated in 1991 [KET91]. These improvements in terms of new features and the development of a number of new techniques are now described.

### 2.A. Apparatus & Techniques

We improved the process that we initially developed in collaboration with Mike Rooks and other staff at the National Nanofabrication Facility at Cornell University [EKP92, KSR91], eventually making 200nm gratings. This required minimizing errors in the electron-beam (e-beam) writer that is used to produce the small scale lines that, with further processing, become our diffraction grating. Since this e-beam machine writes a pattern over a large area by piecing together many small 80  $\mu\text{m}$  by 80  $\mu\text{m}$  fields, mechanical misalignment of the adjacent patterns and thermal drifts in the apparatus which occur during the tens of minutes required to write an entire grating are the predominant sources of error. These barriers to large scale dimensional register — called stitching errors — are an important problem in nanofabrication generally.

During our most recent visit to the NNF in the fall of 1994, we made a further dramatic improvement in our fabrication process by incorporating a preregistering technique. Before the grating lines are written, we now write a series of cross-shaped reference marks at the intersections of the 80  $\mu\text{m}$  fields around the periphery of the grating that can later be "read" as registration marks by the e-beam machine. This procedure can be done very rapidly by the e-beam machine, minimizing the effects of thermal drifts. During the time consuming process of writing the actual grating lines, the e-beam machine is programmed to re-register its position with respect to these crosses. As a result, we have seen atom interference fringes with as much as 49% contrast. (The maximum theoretical contrast for our particular geometry is about 60%.) This verifies that the 200 nm gratings we now use are quite accurate. This solution to the stitching problem is of general interest in nanofabrication, and will be presented at a conference in this area [RTC95].

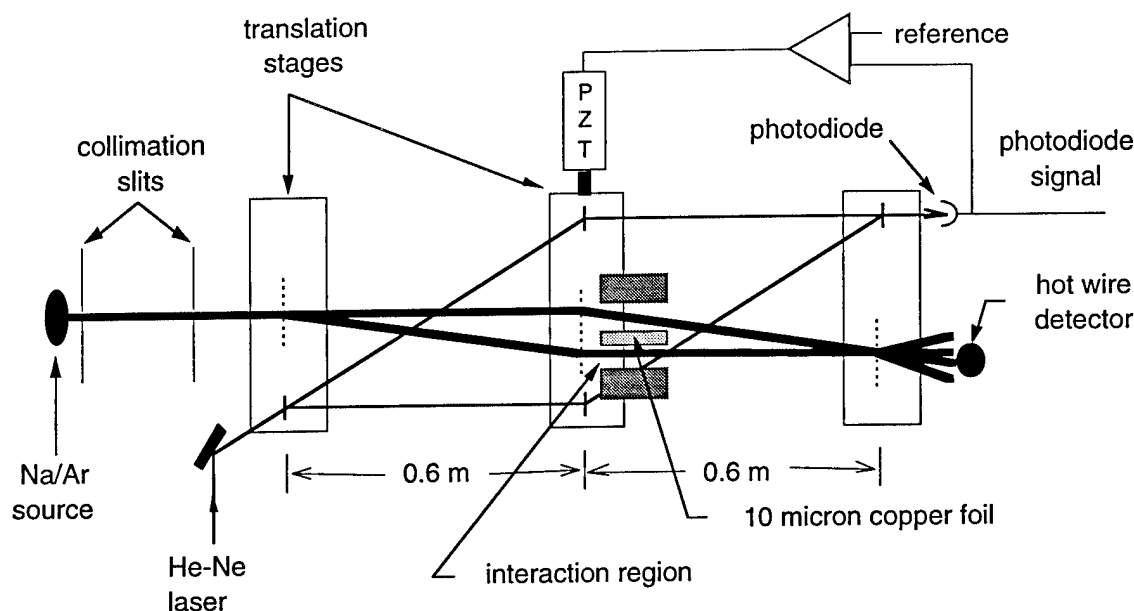


**Figure 1.** A schematic, not to scale, of our atom interferometer (thick lines are atom beams). The 0th and 1st order beams from the first grating strike the middle grating where they are diffracted to form an interference pattern in the plane of the third grating. The detector, located beyond the third grating, records the flux transmitted by the third grating. The 10 cm long interaction region with the 10  $\mu\text{m}$  thick copper foil between the two arms of the interferometer is positioned behind the 2nd grating. An optical interferometer (thin lines are laser beams) measures the relative positions of the 200 nm period atom gratings (which are indicated by vertical dashed lines).

Atom gratings fabricated using our techniques have been used at MPI Goettingen and have been copied by groups at University of Minnesota and Oregon State University. Improvements that we propose here in grating fabrication are therefore likely to find other applications in the AMO and Physical Chemistry communities.

The second new feature that needed to be developed to perform separated beam experiments was a delicate and precise interaction region. We devised a technique to mount a 10  $\mu\text{m}$  thick foil stretched almost perfectly flat over a length of 10 cm. Controlled by a set of linear and rotational manipulators, this foil can be finely positioned between the two beam paths whose edges are separated by only 20  $\mu\text{m}$  (See Figure 1).

The third advance was in the atom beam itself. The sodium (Na) atomic and molecular beams used in our interferometer are now produced by a new supersonic atom source which reliably produces a beam intensity of  $10^{22}$  detected atoms/sec-sr-cm<sup>2</sup>, one of the brightest sources of atoms available. Additionally, we can now polarize this atom beam with light from a cw tunable dye laser and manipulate our atom beam with light forces – both features that allow us to perform new experiments.

Finally, one of the keys to the successful development and use of our separated-beam interferometer during the current grant period was minimizing the contrast reducing vibrations in the machine to a level that permitted the use of 200 nm period gratings. The relative transverse

motions of the gratings must be controlled to within a fraction of the grating period (e.g., within about 40 nm for 200 nm gratings). We accomplished this stabilization with a combination of passive and active control measures. We have gone to great lengths to passively isolate the machine from building noise and mechanical vacuum pump noise. We also employ an active position servo system that uses an optical Mach-Zender interferometer to measure the relative transverse positions of the atom gratings. The optical interference signal is used to apply a correction signal to a piezoelectric transducer on one of the grating translation stages to reduce the uncertainty of the relative position of the atom gratings during the transit time of the atom (~1.3 msec) to ~40 nm rms, as required.

We recently made two further advances in the elimination of vibrations from our apparatus. We now have our apparatus suspended from the ceiling by a cable to isolate it from building noise. This also will facilitate the application of rotations, discussed below. Second, we eliminated a significant source of vibrational noise that had gone previously undetected. The combination of these two advances significantly reduced the residual vibrational noise between the three gratings. We can now routinely observe interference fringes with >40% contrast, compared to the 30-33% contrast that was previously obtained.

## 2.B. Experiments

### 2.B.1. Accurate Atomic Polarizability

In our first experiment, we made a precision measurement of the polarizability ( $\alpha$ ) of the ground state of the sodium atom with an error of 0.35% [ESC95]. This is an improvement by a factor of 20 over previous absolute measurements and challenges the current accuracy level (1%) of theoretical atomic structure calculations. The dramatic increase in accuracy of atomic polarizability achieved here comes from measuring the Stark energy (phase shift) directly rather than by measuring its spatial derivative as in all previous experiments.

We apply a uniform electric field  $\mathcal{E}$  to one of the separated atomic beams, shifting its energy by the Stark potential  $U_{Stark} = -\alpha\mathcal{E}^2/2$ . The resulting phase shift is

$$\Delta\varphi = \frac{1}{\hbar v} \int U_{Stark} dx = \frac{1}{\hbar v} \frac{1}{2} \alpha \left(\frac{V}{D}\right)^2 L_{eff}$$

where  $v$  is the mean velocity of the atomic beam,  $V$  is the voltage applied to one side of the interaction region across a distance  $D$  and  $L_{eff}$  is the effective interaction region length. The induced phase shift is quadratic in the applied potential, as is shown in Fig. 2.B.1. We measured an electric polarizability of  $\alpha=24.11(6)(6) \times 10^{-24} \text{ cm}^3$ , an accuracy of 0.35%. The first error is statistical and is dominated by the uncertainty in the determination of our velocity distribution, the short term stability of the phase reference in our experiment, and to a lesser extent by counting statistics. The second error is systematic and was dominated by uncertainties in measuring the geometry of the interaction region.

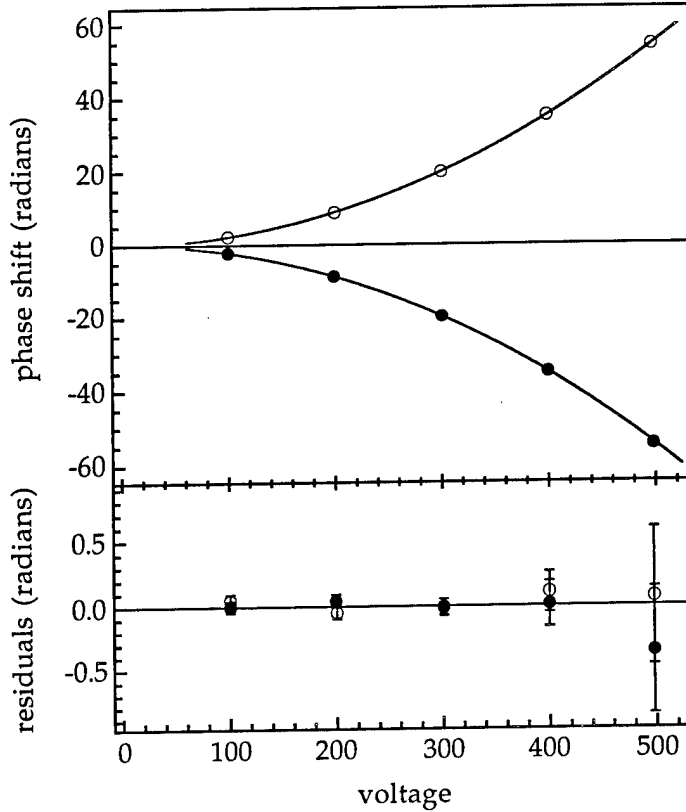


**Figure 2.** Phase shift of the interference pattern as a function of voltage applied to the left (open circles) or right (filled circles) side of the interaction region. The fit is to a quadratic and the residuals are shown in the lower graph.

### 2.B.2. Index of Refraction

We measured the index of refraction of sodium matter waves passing through various gases by inserting a gas cell in one arm of the interferometer [SCE95]. The atom wave passing on the gas-filled side of the interaction region was attenuated and phase shifted in proportion to the gas pressure, resulting in an attenuation and phase shift of the interference pattern at the detector. This experiment solves an old problem in atomic physics: determination of the collision-induced phase shift. Our semiclassical model shows that the phase shift sensitively depends on the shape of the long-range part of the potential between the colliding species. Some of our results have noticeable discrepancies when compared with predictions based on currently accepted potential parameters. These discrepancies reflect the fact that our results are sensitive to the long range form of the potential (rather than its value); it should therefore be possible to find a potential that agrees with all the data.

In analogy with wave optics, the atom's wave function  $\Psi$  while propagating through a medium is given by  $\Psi(x) = \Psi(0)e^{ik_{lab}x} e^{i\frac{2\pi}{k_c}Nx\text{Re}(f(k_c,0))} e^{-\frac{2\pi}{k_c}Nx\text{Im}(f(k_c,0))}$ . Here  $k_{lab}$  is the wave vector in the laboratory frame,  $k_c$  the wave vector in the center of mass frame of the collision,  $N$  is the column density of the medium and  $f(k_c,0)$  is the forward scattering amplitude. When this wave interferes with the unattenuated wave, the amplitude of the resulting interference pattern is attenuated in proportion to the imaginary part of the forward scattering amplitude and phase shifted in proportion to the real part of the forward scattering amplitude. The ratio of these quantities is accurately determined from the slope of the phase shift plotted as a function of the natural logarithm of the interfering amplitude (Fig. 2.B.2.). Since both the attenuation and phase shift can simultaneously be determined from the same interference scan, this method does not rely on a pressure measurement at all. We measured this ratio for the various monatomic rare gases He, Ne, Ar, Kr, Xe and for the molecular gases  $N_2$ ,  $CO_2$ ,  $NH_3$  and  $H_2O$ . It is noteworthy that the measured phase shifts as a function of gas pressure vary by a factor of 13 and thus are a more sensitive probe of the interatomic potential than the total scattering cross sections, which vary only by a factor of 4.

We found semi-classical analytical solutions for  $\text{Re}(f(k,0)) / \text{Im}(f(k,0))$  for a hard sphere and for long range interatomic potentials with the form  $r^{-n}$ . We find that the ratio is sensitively dependent on  $n$ . We find that helium behaves most like a hard sphere, which is consistent with

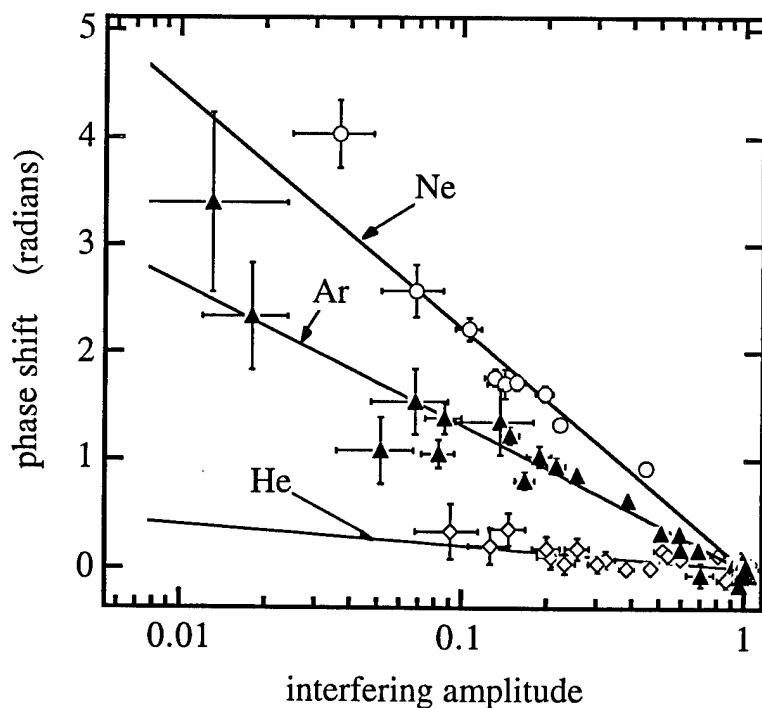


**Figure 3.** Phase shift of Na matter waves plotted vs. the interfering amplitude when passing through He, Ne and Ar in the gas cell. The slope of the fitted line is a direct measurement of the ratio  $\text{Re}(f(k,0)) / \text{Im}(f(k,0))$ .

the fact that it has the weakest long range attraction and a very shallow minimum. The Na-Xe potential, on the other hand, has a deep well, so the long range part of the potential should be well represented by an  $r^{-n}$  form. Its ratio comes closest to the value we predict for the expected long range  $r^{-6}$  interaction. The values measured for the other gases decrease progressively further from this ratio as the well depth decreases (which it does monotonically with decreasing mass of the rare gas), with Ne being abnormally high due to its shallow well.

### 2.B.3. Molecule Interferometry

Recently we have developed techniques to perform interferometry with molecule beams, and have applied them to measure the index of refraction (in the manner of the above experiment) with molecular de Broglie waves. We first developed techniques to produce an intense, pure beam of sodium dimers ( $\text{Na}_2$ ) using light forces to separate the atomic and molecular species in a seeded supersonic beam. We used diffraction from a micro-fabricated grating to study the atomic and molecular sodium in the beam and to verify that, in fact, a pure  $\text{Na}_2$  beam was generated.

Using krypton carrier gas to slow the molecules as much as possible and increase the diffraction angle correspondingly, we showed that our atom interferometer produced high contrast  $\text{Na}_2$  fringes and was able to physically separate the molecule waves in the interaction region. We measured the attenuation and phase shift of  $\text{Na}_2$  molecular de Broglie waves scattering from neon by putting this gas on one side of the interaction region used in the above experiment. This experiment raises interesting quantum mechanical issues concerning the possible limitations for observing interference with complex particles, such as a particle's size or its large number of unselected internal states - here shown to be no barrier to interferometry.

### 2.B.4. Contrast Interferometry

We have developed a new type of interferometry in which information is derived from oscillations in the contrast of the interference pattern rather than its phase. This effect [SEC94] arises because sodium has eight different magnetic ground states in its hyperfine structure, each with its own Zeeman energy  $U(x) = -\vec{\mu} \cdot \vec{B} = g_F \mu_B m_F B$  that determines the phase shift of its interference pattern. The total interference pattern will be the incoherent sum of the individual interference patterns for the various states. We demonstrated that contrast oscillations arise from the interplay of these different interference patterns. Sharp revival peaks are observed because all the components in the interference pattern are shifted by an integer multiple of  $g_F \mu_B BL / \hbar v$  and therefore rephase when this quantity is an integer multiple of  $2\pi$ , accurately determining  $g_F \mu_B BL / \hbar v$ .

This technique can be applied in several ways. If the interaction is accurately known, as in the case above, we can measure the velocity distribution independently. On the other hand this rephasing technique can be applied to other systems, such as molecules, where the interaction strength differs (e.g. due to dependence on unselected quantum numbers) for different particles in the interferometer, making it possible to measure properties such as tensor polarizabilities. We also showed that we can use this technique in conjunction with a large Stark shift to isolate the interference signal from one magnetic state, allowing us to perform experiments with polarized atoms even though the beam as a whole is unpolarized.

### 2.B.5. Decoherence experiment

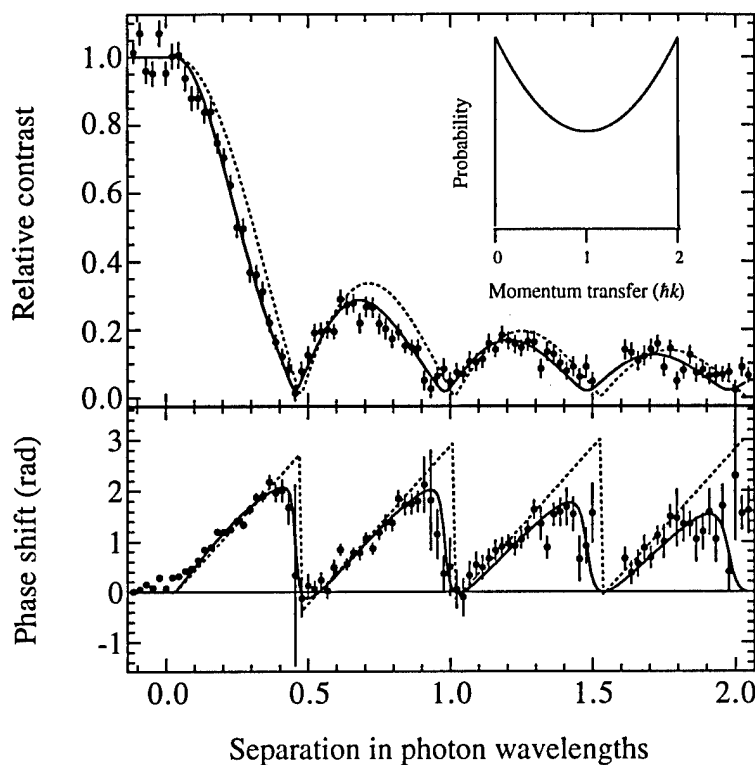


**Figure 4.** Relative contrast and phase shift of the IFM as a function of the separation of the IFM arms at the point of scattering. The inset shows the angular distribution of spontaneously emitted photons projected onto the  $x$  axis. The dashed curve corresponds to purely single photon scattering, and the solid curve is a best fit that includes contributions from atoms that scattered 0 photons (4%) and 2 photons (14%).

We have recently completed a study of the decoherence effects due to photon scattering from the atoms in the interferometer [CHL95]. It is generally assumed that the spontaneous emission of a photon will destroy atomic coherence due to the random phase of the photon. A closer look shows that this is not necessarily the case. Consider the whole process as a “welcher weg” (which-way) experiment, in which we try to determine which path the atom took in the interferometer. If the two paths are separated by much more than the wavelength of the emitted photon, in principle we can determine the path from which the photon came by observing it with a microscope, implying the absence of interference. If the separation is so small that this cannot be determined, the interference pattern should not necessarily be destroyed.

We have quantitatively studied this induced loss of interference as a function of the mean separation,  $d$ , of the interfering atomic wavefunction by scattering single photons at various locations within the interferometer. To describe these effects, consider an atom within the interferometer that elastically scatters a photon with a well-defined incident and final

momentum,  $\vec{k}_i$  and  $\vec{k}_f$  with  $|\vec{k}_i| = |\vec{k}_f|$ . Before the scattering, the combined atom-photon wave function is separable and may be written  $|\psi\rangle_i \propto [\varphi_u(x) + \varphi_l(x)] \otimes |\vec{k}_i\rangle$ , where  $\varphi_u(x) + \varphi_l(x)$  refer to the upper and lower arms of the interferometer. After the scattering, the combined wavefunction is entangled and we have

$$|\psi\rangle_f \propto [\varphi_u(x - \Delta x) + e^{i\Delta\phi} \varphi_l(x - \Delta x)] \otimes |\vec{k}_f\rangle$$

where  $\Delta\vec{k} = \vec{k}_f - \vec{k}_i$ . The shift  $\Delta x$  is due to the momentum transfer to the atom and represents a shift of the fringe envelope at the plane of the third grating. Additionally, there is a relative phase shift produced by the atom-photon interaction  $\Delta\phi = \Delta\vec{k} \cdot \vec{d} = \Delta k_x d$  where  $d$  is the spatial separation of the two arms of the interferometer (proportional to the distance past the first grating), and  $\Delta k_x$  is the component of momentum transfer along  $x$ . The resulting fringe pattern is given by an incoherent sum of interference patterns with different phase shifts weighted according to the angular distribution of emitted photons  $P(\Delta k_x)$ . This is similar to the theoretical results obtained for the Young's double slit experiment [SCP91, TAW93].

The experimental results show that, as expected, scattering the photons before or *immediately* after the first grating does not effect the contrast or the phase of the interferometer. For small beam separations, the phase of the interferometer increases linearly with  $d$  with a slope determined by the average momentum transfer of  $1\hbar k$ . The contrast decreases sharply as  $d$  increases and falls to zero for a separation of about half the photon wavelength. As the separation is increased, there are periodic revivals of the contrast and a periodic phase modulation.

### 2.B.6. Regained coherence through greater selectivity

The loss of interference contrast in the above experiment is due to a combination of the entanglement between the atoms and the photons and the fact that the final state of the photon is not observed. The resulting uncertainty in the state of this small reservoir of incoherence is responsible for the loss of coherence. If we only detected atoms which left the reservoir in a particular state, i.e. with scattered single photons into a particular  $\vec{k}_f$ , we would expect each atom to have the same phase shift  $\Delta\phi$  and displacement of the envelope of its fringes, both proportional to  $\Delta k_x$ . Interference patterns from these selected atoms would add in phase with no loss in contrast. Therefore it is, in principle, possible to recover the contrast in the final interference pattern by observing only those atoms entangled with photons scattered in a particular direction. This could be achieved experimentally by observing atoms in coincidence with photons scattered in that direction. Unfortunately, such an experiment is not realistically achievable in our apparatus for a number of technical reasons, mainly the long response time of the atom detector and the inefficiency of detecting photons.

However, we devised a unique experimental realization of such a correlation experiment that exploits the fact that the envelope of the fringes of atoms which have scattered photons with a particular  $\Delta k_x$  is shifted by the recoil momentum from scattering the photon (i.e. by  $\hbar\Delta k_x$ ) [CHL95]. By using very narrow atomic beam collimation (10  $\mu\text{m}$  slits instead of 40 $\mu\text{m}$ ) in conjunction with a correspondingly reduced detector acceptance (10 $\mu\text{m}$  wide instead of 50 $\mu\text{m}$ ), we have selectively detected only atoms which are correlated with photons scattered within a limited  $\Delta k_x$ . We performed the experiment for several different values of  $\Delta k_x$ . We call this "regained coherence" since a substantial amount of contrast is regained at the position of the first

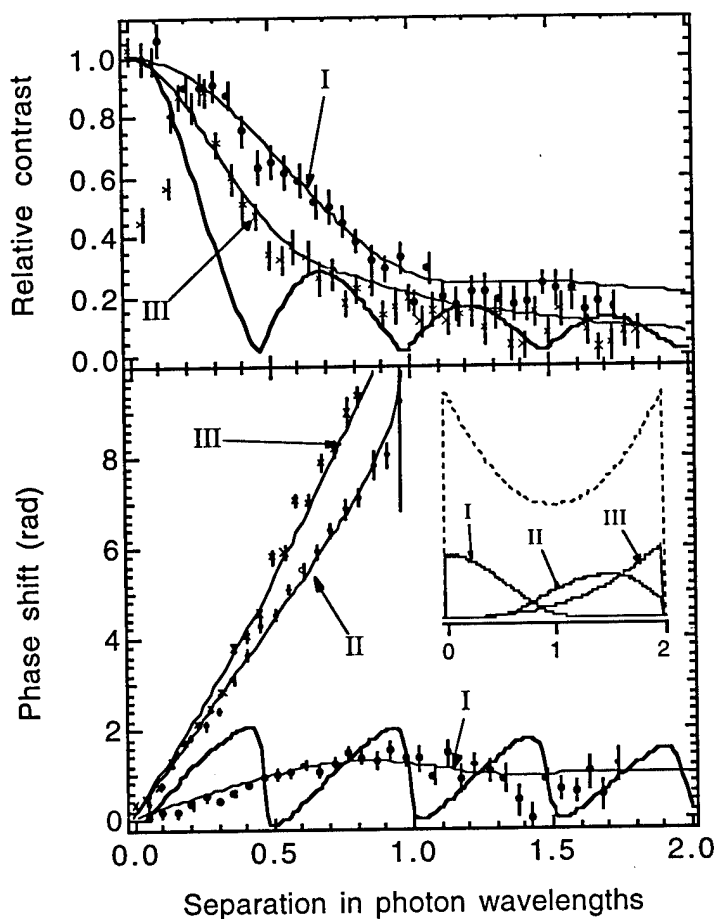


**Figure 5.** Relative contrast and phase shift of the IFM as a function of  $d$  for the cases in which atoms are correlated with photons scattered into a limited range of directions. The dashed curve is for the uncorrelated case. The inset shows the acceptance of the detector for each case compared to the original distribution (dotted line). Case I corresponds to predominantly forward scattered photons (minimal transfer of momentum), case III corresponds to backward scattered photons (transfer of 2 photon momenta), and case II lies in between.

contrast zero in the decoherence data. We have also demonstrated that the average phase shift of the atom interference pattern has a slope that is strongly dependent on  $\Delta k_x$ . We believe that this experiment is a classic in the study of quantum decoherence, and is closely related to modern discussions of quantum measurement theory.

### 3. Publications and Theses

#### 3.A. Recent papers published or submitted:

- [CHL95] Photon Scattering from Atoms in an Atom Interferometer: Coherence Lost and Regained, M.S. Chapman, T.D. Hammond, A. Lenef, J. Schmiedmayer, R.A. Rubenstein, E.T. Smith, D.E. Pritchard, Submitted to Phys. Rev. Lett.
- [RTC95] Coherence of large gratings and electron-beam fabrication techniques for atom-wave interferometry, M.J. Rooks, R.C. Tiberio, M.S. Chapman, T.D. Hammond, E.T. Smith, A. Lenef, R. Rubenstein, D. Pritchard, S. Adams, Submitted to J. Vac. Sci. Technol. B.
- [CEH95a] Optics and Interferometry with Molecules, Michael S. Chapman, C. R. Ekstrom, T. D. Hammond, R. Rubenstein, J. Schmiedmayer, S. Wehinger, D.E. Pritchard, Phys. Rev. Lett. **74**, 4783 (1995)
- [CEH95b] Near Field Imaging of Atom Diffraction Gratings: the Atomic Talbot Effect, M. S. Chapman, C.R. Ekstrom, T.D. Hammond, J. Schmiedmayer, B.E. Tannian, S. Wehinger and D.E. Pritchard, Phys. Rev. A **51**, R14 (1995).
- [ESC95] Measurement of the Electric Polarizability of Sodium with an Atom Interferometer, C. R. Ekstrom, J. Schmiedmayer, M.S. Chapman, T.D. Hammond, and D.E. Pritchard, Phys. Rev. A **51**, 3883 (1995).
- [HPC95] Multiplex Velocity Selection for Precision Matter Wave Interferometry, T. D. Hammond, D.E. Pritchard, M.S. Chapman, A. Lenef, and J. Schmiedmayer, App. Phys. B **60**, 193 (1995).
- [SCE95] Index of Refraction of Various Gases for Sodium Matter Waves, J. Schmiedmayer M.S. Chapman, C.R. Ekstrom, T.D. Hammond, S. Wehinger and D.E. Pritchard, Phys. Rev. Lett. **74**, 1043 (1995).
- [PCE94] Interferometry with Atoms and Molecules, D. E. Pritchard, M. S. Chapman, C. R. Ekstrom, T. D. Hammond, J. Schmiedmayer, A. Lenef, R. Rubenstein, and S. Wehinger, in Fundamental Problems in Quantum Theory, Proc. of the New York Academy of Sciences, Baltimore, MD, June 18 - 22, 1994 (New York Academy of Sciences, New York, 1995).
- [PRI94] Atom Optics, David E. Pritchard, McGraw-Hill Encyclopedia of Physics, 1994.
- [SEC94] Magnetic Coherences in Atom Interferometry, J. Schmiedmayer, C.R. Ekstrom, M.S. Chapman, T.D. Hammond, S. Wehinger and D.E. Pritchard, J. Phys. II (France) **4**, 2029 (1994).
- [ESC93] Experiments with a Separated-Beam Atom Interferometer, C. R. Ekstrom, J. Schmiedmayer, M. S. Chapman, T. D. Hammond, and D. E. Pritchard, Proceedings QELS May 2-7, Baltimore, Md 1993.

- [PES93] Atom Interferometry, D. E. Pritchard, C. R. Ekstrom, J. Schmiedmayer, M. S. Chapman, and T. D. Hammond, In Proceedings of the Eleventh International Conference on Laser Spectroscopy, June 13- 18, 1993, Editors, L. A. Bloomfield, T. F. Gallagher, and D. J. Larson. (American Institute of Physics, New York, 1993).
- [PHS93] Atom Interferometry, D. E. Pritchard, T. D. Hammond, J. Schmiedmayer, C. R. Ekstrom, and M. S. Chapman, In Proceedings of the Conference on Quantum Interferometry, Trieste, Italy, March 2-5, 1993, Eds., F. DeMartini, A. Zeilinger, and G. Denardo. (World Scientific, Singapore, 1993).
- [PRI93] Atom Interferometers, D. E. Pritchard, In Proceedings of the 13th International Conference on Atomic Physics, Munich, Germany, August 3-7, 1992, Editors, T. W. Hansch, H. Walther, and B. Neizert, (American Institute of Physics, New York, 1993).
- [SEC93] Atom Interferometry, J. Schmiedmayer, C. R. Ekstrom, M. S. Chapman, T. D. Hammond, and D. E. Pritchard, In Proceedings, Seminar on Fundamentals of Quantum Optics III, Kuhtai, Austria, 1993, Ed. F. Ehlötzky, (Springer-Verlag, Berlin).
- [EKP92] Atom Optics using Microfabricated Structures, C. R. Ekstrom, D. W. Keith, and D. E. Pritchard, *App. Phys. B* **54**, 369 (1992).
- [PRI92] Atom Interferometers, D. W. Pritchard, In Proceedings of the International conference on the Fundamental Aspects of Quantum Theory, Univerisity of South Carolina, December, 1992. (World Scientific, Singapore).
- [TPK92] Numerical Model of a Multiple Grating Interferomter, Q. A. Turchette, D. E. Pritchard, and D. W. Keith, *JOSA-B* **9**, 1601 (1992).

### 3.B. Thesis:

Thesis, Ph.D.: M. Chapman, "Photon Induced Coherence Loss in Atom Interferometry," Dept. of Physics, MIT, 1995.

Thesis, Ph. D.: C. Ekstrom, "Experiments with a Separated Beam Atom Interferometer," Dept. of Physics, MIT, 1993.

Thesis, B. S.: Bridget E. Tannian, "Near-Field Imaging of Atom Diffraction Gratings: the Atomic Talbot Effect," Dept. of Physics, MIT, 1994.

## 4. Scientific Personnel

### PROFESSORS

David E. Pritchard, Prof. of Physics, Massachusetts Institute of Technology

### GRADUATE STUDENTS

Michael S. Chapman

Christopher R. Ekstrom

Troy D. Hammond

Richard A. Rubenstein

Edward T. Smith

### UNDERGRADUATE STUDENTS

Bridget E. Tannian

Quentin A. Turchette.

### VISITORS AND POSTDOCS

Herbert Bernstein - professor at Amherst Univerisity

Alan Lenef - current postdoc

Jörg Schmiedmayer - permanent position at University of Innsbruck

Stephan Wehinger - graduate student from University of Innsbruck

### Prizes, honors, and theses of supported personnel:

California Institute of Technology Milliken postdoctoral fellowship (1995) - Michael Chapman

National Science Foundation Graduate Fellowship ( 1992 - 1995) - Edward Smith

Austrian Academy of Sciences Fellowship (1995) - Jörg Schmiedmayer

Election to Fellow of American Academy of Arts and Sciences (1994) - David E. Pritchard

Erwin Schrödinger fellowship from the Austrian Academy of Sciences (1992 - 1994) - Jörg Schmiedmayer

Alexander von Humboldt postdoctoral fellowship (1993) - Christopher Ekstrom

National Science Foundation Graduate Fellowship (1990 - 1993) - Troy Hammond

Distinguished Traveling Lecturer of Laser Science Topical Group to the American Physical Society (1991 - 1993) - David E. Pritchard

## 6. Bibliography

- [ASM94] See the recent review of atom optics by C.S. Adams, M. Sigel and J. Mlynek, Phys. Rep. **240**, 143 (1994) .
- [CAM91] O. Carnal and J. Mlynek, Phys. Rev. Lett. **66**, 2689 (1991) .
- [CHL95] M.S. Chapman *et al.*, Phys. Rev. Lett. (1995) submitted.
- [EKP92] C.R. Ekstrom, D.W. Keith and D.E. Pritchard, App. Phys. B **54**, 369 (1992) .
- [ESC95] C.R. Ekstrom, J. Schmiedmayer, M.S. Chapman, T.D. Hammond and D.E. Pritchard, Phys. Rev. A **51**, 3883 (1995) .
- [KAC91] M. Kasevich and S. Chu, Phys. Rev. Lett. **67**, 181 (1991) .
- [KET91] D.W. Keith, C.R. Ekstrom, Q.A. Turchette and D.E. Pritchard, Phys. Rev. Lett. **66**, 2693 (1991) .
- [KSR91] D.W. Keith, R.J. Soave and M.J. Rooks, J. Vac. Sci. Technol. B **9**, 2846 (1991) .
- [RKW91] F. Riehle, T. Kisters, A. Witte, J. Helmcke and C.J. Bordé, Phys. Rev. Lett. **67**, 177 (1991) .
- [RTC95] M.J. Rooks *et al.*, J. Vac. Sci. Technol. B submitted.
- [SCE95] J. Schmiedmayer, M.S. Chapman, C.R. Ekstrom, T.D. Hammond, S. Wehinger and D.E. Pritchard, Phys. Rev. Lett. **74**, 1043 (1995) .
- [SCP91] T. Sleator, O. Carnal, T. Pfau, A. Faulstich, H. Takuma and J. Mlynek. in *Laser Spectroscopy X*, p. 264, edited by M. Dulcoy, E. Giacobino and G. Camy (World Scientific, Singapore, 1991).
- [SEC94] J. Schmiedmayer, C.R. Ekstrom, M.S. Chapman, T.D. Hammond and D.E. Pritchard, J. Phys. II France **4**, 2029 (1994) .
- [TAW93] S.M. Tan and D.F. Walls, Phys. Rev. A **47**, 4663 (1993) .